

# The search for magnetic fields in two Wolf-Rayet stars and the discovery of a variable magnetic field in WR 55

S. Hubrig<sup>1</sup>†, M. Schöller<sup>2</sup>, A. Cikota<sup>3</sup>, S. P. Järvinen<sup>1</sup>

<sup>1</sup>*Leibniz-Institut für Astrophysik Potsdam (AIP), An der Sternwarte 16, 14482 Potsdam, Germany*

<sup>2</sup>*European Southern Observatory, Karl-Schwarzschild-Str. 2, 85748 Garching, Germany*

<sup>3</sup>*Physics Division, E.O. Lawrence Berkeley National Laboratory, 1 Cyclotron Road, Berkeley, CA 94720, USA*

Accepted XXX. Received YYY; in original form ZZZ

## ABSTRACT

Magnetic fields in Wolf-Rayet (WR) stars are not well explored, although there is indirect evidence, e.g. from spectral variability and X-ray emission, that magnetic fields should be present in these stars. Being in an advanced stage of their evolution, WR stars have lost their hydrogen envelope, but their dense winds make the stellar core almost unobservable. To substantiate the expectations on the presence of magnetic fields in the most-evolved massive stars, we selected two WR stars, WR 46 and WR 55, for the search of the presence of magnetic fields using FORS2 spectropolarimetric observations. We achieve a formally definite detection of a variable mean longitudinal magnetic field of the order of a few hundred Gauss in WR 55. The field detection in this star, which is associated with the ring nebula RCW 78 and the molecular environment, is of exceptional importance for our understanding of star formation. No field detection at a significance level of  $3\sigma$  was achieved for WR 46, but the variability of the measured field strengths can be rather well phased with the rotation period of 15.5 h previously suggested by FUSE observations.

**Key words:** techniques: polarimetric — stars: individual: WR 46 — stars: individual: WR 55 — stars: magnetic fields — stars: massive — stars: Wolf-Rayet

## 1 INTRODUCTION

In the modeling of massive stars, specific aspects, especially the role of magnetic fields, remain not well understood, implying large uncertainties in the star’s evolutionary path and ultimate fate. Previous observations indicate that probably about 7% of O-type stars with masses exceeding  $18 M_{\odot}$  and about 6% of early B- and O-type stars have measurable, mostly dipolar magnetic fields (e.g., Grunhut et al. 2017; Schöller et al. 2017). Theoretical models suggest that O stars with strong magnetic field detections may be related to magnetars with  $B \approx 10^{15}$  G (e.g. Thompson et al. 2004). Thus, it is important to detect magnetic fields in WR stars, which are descendants of massive O stars and direct predecessors of compact remnants. WR stars are highly chemically evolved massive stars that have lost their hydrogen envelope and now expose their former stellar core. However, their dense winds make the stellar surface almost unobservable.

Magnetic fields in WR stars are currently not sufficiently explored, in spite of the fact that there is indirect evidence, e.g. from spectral variability and X-ray emission, that magnetic fields are present in WR star atmospheres (e.g. Michaux et al. 2014). Previous theoretical work of Gayley & Ignace (2010) predicted a fractional circular polarization of a few times  $10^{-4}$  for magnetic fields of

about 100 G. Using high-resolution spectropolarimetric observations with ESPaDOnS at the Canada–France–Hawaii Telescope, de la Chevrotière et al. (2014), reported marginal magnetic field detections for WR 134, WR 137, and WR 138, corresponding to magnetic field strengths of about 200 G, 130 G, and 80 G, respectively, and an average upper limit of about 500 G for the non-detections in other stars. As the line spectrum in WR stars is formed in the strong stellar wind, the detection of magnetic fields in these stars is difficult. The major problem is the wind broadening of the emission lines by Doppler shifts with wind velocities of a few thousand  $\text{km s}^{-1}$ . The broad spectral lines observed with high-resolution spectropolarimetry extend over adjacent orders, so that it is necessary to adopt order shapes to get the best continuum normalization.

Because of such immense line broadening in WR stars, to search for weak magnetic fields in a number of WR stars, Hubrig et al. (2016) used the FOcal Reducer low dispersion Spectrograph in spectropolarimetric mode (FORS2; Appenzeller et al. 1998) mounted on the 8 m Antu telescope of the European Southern Observatory’s Very Large Telescope (VLT) on Cerro Paranal/Chile. The obtained FORS2 polarimetric spectra allowed Hubrig et al. (2016) to measure the mean longitudinal magnetic field  $\langle B_z \rangle = 258 \pm 78$  G in the cyclically variable and X-ray emitting WN5 star WR 6 at a significance level of  $3.3\sigma$ . Keeping in mind that the two clearly magnetic Of?p stars HD 148937 and CPD  $-28^{\circ}$  5104

† Corresponding author: shubrig@aip.de

were for the first time detected as magnetic in the FORS2 observations at significance levels of  $3.1\sigma$  and  $3.2\sigma$ , respectively (Hubrig et al. 2008, 2011), the detection of the magnetic field in WR 6 at a significance level of  $3.3\sigma$  indicates that a magnetic field is likely present in this star. Spectropolarimetric monitoring of WR 6 revealed a sinusoidal nature of the  $\langle B_z \rangle$  variations, which is indicative of a predominantly dipolar magnetic field structure (Hubrig et al. 2016; see Fig. 1, left side). The field appeared to be reversing, with the extrema detected at rotation phases 0 and 0.5.

In the sample of spectropolarimetrically studied WR stars by Hubrig et al. (2016), WR 6 was the only target showing X-ray emission and cyclical variability due to the presence of corotating interacting regions (CIRs), which are formed out of the interaction between high and low-velocity flows as the star rotates (e.g. St-Louis et al. 1995). CIRs were detected in spectroscopic time series observations of only a few massive stars (e.g. Mullan 1984). It was suggested that CIRs are related to the presence of magnetic bright spots, which are indicators of the presence of a global magnetic field (e.g. Ramiaramanantsoa et al. 2014)

To substantiate expectations on the presence of magnetic fields in the most-evolved massive stars, we have searched for magnetic fields in two other promising targets, WR 46 (=HD 104994) and WR 55 (=HD 117688), which, similar to WR 6, show CIRs (e.g. Chené & St-Louis 2011). These stars are accessible from the VLT and have never been observed with spectropolarimetry in the past.

WR 46 is a WN3p star (Hamann et al. 2019), with relatively strong O IV  $\lambda$  3811 and  $\lambda$  3834 emission lines. It is very hot and compact ( $T_{\text{eff}} = 112.2 \text{ kK}$ ,  $R = 1.4 R_{\odot}$ ), and also bright in X-rays, possessing a hard component in its X-ray emission (Gosset et al. 2011), which may indicate the magnetic nature of WR 46. According to Hénault-Brunet et al. (2011), WR 46 is known to exhibit a very complex variability pattern. The different periods and timescales observed in the past suggest the presence of multiple periods, including dominant and secondary periods (see Fig. 1 in their work). To explain the short-term variability of this star, various scenarios were evoked, including the possibility of a close binary or non-radial pulsations (e.g. Veen et al. 2002a,b). Using observations with the Far Ultraviolet Spectroscopic Explorer (FUSE), Hénault-Brunet et al. (2011) found significant variations on a timescale of  $\sim 8 \text{ h}$ . This period is close to the photometric and spectroscopic periods previously reported by other authors. Hénault-Brunet et al. (2011) also reported the detection of a second significant peak, just slightly weaker, corresponding to  $P = 15.5 \pm 2.5 \text{ h}$ .

WR 55 is a significantly cooler ( $T_{\text{eff}} = 56.2 \text{ kK}$ ) WN7 star with hydrogen deficiency and belongs to the WNE subclass, like WR 6 (Hamann et al. 2006). However, its radius,  $R = 5.2 R_{\odot}$ , is larger compared to the radius of WR 6 with  $R = 3.2 R_{\odot}$ . A highly significant level of spectroscopic variability of about 10% was discovered by Chené & St-Louis (2011). So far, no periodicity search was carried out for this star. Cappa et al. (2009) investigated the distribution of molecular gas related to the ring nebula RCW 78 around WR 55 and concluded that WR 55 is not only responsible for the ionization of the gas in the nebula, but also for the creation of the interstellar bubble. Their analysis indicates that the star formation in this region is induced by the strong wind

of this star. Thus, the discovery of a magnetic field in WR 55 would be of exceptional interest for star formation theories.

As WR stars are characterized by spectra showing very broad emission lines, the determination of their magnetic fields is usually based on the calculation of the mean longitudinal magnetic field, i.e. of the line-of-sight field component, using circularly polarized light. To search for magnetic fields in WR 46 and WR 55, we obtained several randomly timed distributed low-resolution spectropolarimetric observations using the FOcal Reducer low dispersion Spectrograph (FORS2; Appenzeller et al. 1998), installed at the ESO/VLT. In the following, we give an overview of our spectropolarimetric observations, describe the data reduction and discuss the results of the magnetic field measurements.

## 2 DATA REDUCTION AND RESULTS OF THE MAGNETIC FIELD MEASUREMENTS

To maximize the field detection probability and to avoid missing the magnetic field due to an unfavorable viewing angle in certain rotation phases, FORS2 observations of both targets were obtained on several different epochs to sample different rotation phases. Seven spectropolarimetric observations of WR 46 were obtained in service mode, one observation on 2016 March 14 and six observations from 2020 January 16 to February 21. For WR 55, we obtained five observations from 2020 February 13 to March 10. The last observation of WR 55 recorded on March 10 was not completed, probably due to bad weather conditions, and was therefore used only for the inspection of spectral variability.

The FORS2 multi-mode instrument is equipped with polarisation analysing optics comprising super-achromatic half-wave and quarter-wave phase retarder plates, and a Wollaston prism with a beam divergence of  $22''$  in standard resolution mode. We used the GRISM 600B and the narrowest available slit width of  $0''.4$  to obtain a spectral resolving power of  $R \sim 2000$  in the observed spectral range from 3250 to 6215 Å. For the observations, we used a non-standard read-out mode with low gain (200kHz,  $1 \times 1$ , low), which provides a broader dynamic range, hence allowed us to reach a higher signal-to-noise ratio ( $S/N$ ) in the individual spectra. The circular polarization observations were carried out using a sequence of positions of the quarter-wave plate  $-45^\circ$ ,  $+45^\circ$ ,  $+45^\circ$ ,  $-45^\circ$  and so forth, to minimize the cross-talk effect and to cancel errors from different transmission properties of the two polarized beams. Moreover, the reversal of the quarter-wave plate compensates for fixed errors in the relative wavelength calibrations of the two polarized spectra. The ordinary and extraordinary beams were extracted using standard IRAF procedures as described by Cikota et al. (2017). The wavelength calibration was carried out using He-Ne-Ar arc lamp exposures.

The spectral appearance of the WN stars WR 46 and WR 55 in the FORS 2 spectra is presented in Fig. 1. The spectra of WN stars are dominated by helium and nitrogen lines. The WN3p star WR 46 is characterized by the presence of strong N V and He II lines and the absence of hydrogen. The ‘‘p’’ stands for peculiar and denotes the presence of unusually strong O VI  $\lambda$  3811 and  $\lambda$  3834 emission lines, the relatively strong N V  $\lambda$  4604 line, and relatively weak C IV  $\lambda$  5801 and  $\lambda$  5812 lines (e.g. Conti & Massey 1989).

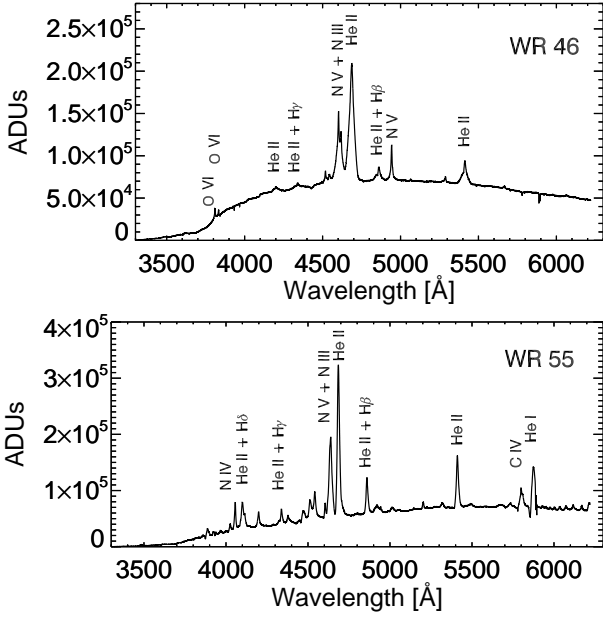


**Figure 1.** FORS 2 Stokes  $I$  spectra of WR 46 and WR 55. Spectral line identification is based on the work of Hamann et al. (2006) and is shown above the line profiles.

While previous observations of WR46 clearly showed the presence of variability in photometry and spectroscopy, the variability of WR55 was studied only once by Chené & St-Louis (2011) using spectra in the spectral range 5200–6000 Å obtained with the 1.5 m telescope of the Cerro Tololo Inter-American Observatory. The authors reported for this star a highly significant level of variability of up to 10% of the line intensity. As we show in Fig. 2, spectral line variability is also detected in our FORS 2 Stokes  $I$  spectra of this star.

A description of the assessment of the presence of a longitudinal magnetic field using FORS1/2 spectropolarimetric observations was presented in our previous work (e.g. Hubrig et al. 2004a,b, and references therein). Improvements to the methods used, including  $V/I$  spectral rectification and clipping, were detailed by Hubrig et al. (2014). Null spectra are calculated as pairwise differences from all available  $V$  profiles so that the real polarisation signal should cancel out. From these,  $3\sigma$ -outliers are identified and used to clip the  $V$  profiles. This removes spurious signals, which mostly come from cosmic rays, and also reduces the noise.

The mean longitudinal magnetic field  $\langle B_z \rangle$  is measured on the rectified and clipped spectra, based on the relation following the method suggested by Angel & Landstreet (1970):

$$\frac{V}{I} = -\frac{g_{\text{eff}} e \lambda^2}{4\pi m_e c^2} \frac{1}{I} \frac{dI}{d\lambda} \langle B_z \rangle, \quad (1)$$

where  $V$  is the Stokes parameter that measures the circular polarization,  $I$  is the intensity in the unpolarized spectrum,  $g_{\text{eff}}$  is the effective Landé factor,  $e$  is the electron charge,  $\lambda$  is the wavelength,  $m_e$  is the electron mass,  $c$  is the speed of light,  $dI/d\lambda$  is the wavelength derivative of Stokes  $I$ , and  $\langle B_z \rangle$  is the mean longitudinal (line-of-sight) magnetic field.

Furthermore, we have carried out Monte Carlo bootstrapping tests. These are most often applied with the pur-

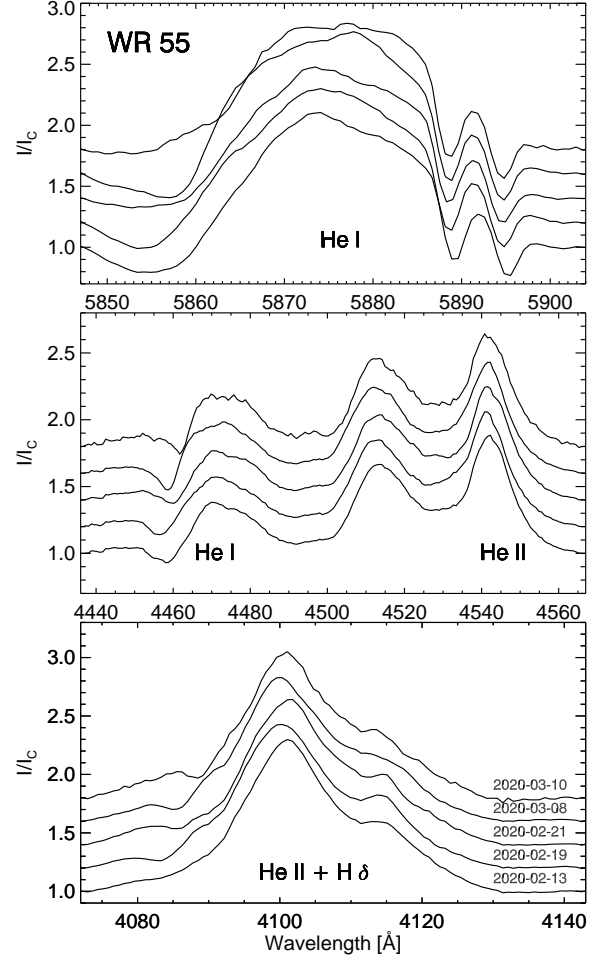


**Figure 2.** FORS 2 Stokes  $I$  spectra showing variability of different spectral lines. The spectra obtained at different epochs are offset vertically for better visibility. Spectral line identification is based on the work of Hamann et al. (2006).

pose of deriving robust estimates of standard errors (e.g. Steffen et al. 2014). The measurement uncertainties obtained before and after the Monte Carlo bootstrapping tests were found to be in close agreement, indicating the absence of reduction flaws. The results of our magnetic field measurements are presented in Table 1.

For WR 46, the values for the longitudinal magnetic field  $\langle B_z \rangle$  show change of polarity, with the strongest mean longitudinal magnetic field of positive polarity  $\langle B_z \rangle = 342 \pm 154$  G at a significance level of  $2.2\sigma$  and the strongest field of negative polarity  $\langle B_z \rangle = -199 \pm 88$  G at a significance level of  $2.3\sigma$ . Since significant photometric and spectroscopic variations on a timescale of  $\sim 8$  h were reported in previous studies of this star, assuming that this periodicity is caused by rotational modulation, we tested the distribution of the measurement values over this period. We do not find any hint for sinusoidal modulation, which is expected for a large-scale organized dipole field structure. However, as we show in Fig. 3, rotation modulation is indicated in our data, if we use the period of 15.5 h suggested by Hénault-Brunet et al. (2011). Due to the large uncertainty of this period, only the measurements obtained in 2020 are fitted by a sinusoid. The older measurement obtained in 2016 and marked by the filled

**Table 1.** Longitudinal magnetic field values obtained for WR 46 and WR 55 using FORS 2 observations. In the first column we show the modified Julian dates of mid-exposures, followed by the corresponding signal-to-noise ratio ( $S/N$ ) of the FORS 2 Stokes  $I$  spectra measured close to 4686 Å. The measurements of the mean longitudinal magnetic field using the Monte Carlo bootstrapping test and using the null spectra are presented in Columns 3 and 4. All quoted errors are  $1\sigma$  uncertainties.

MJD	$S/N$	$\langle B_z \rangle$ (G)	$\langle B_z \rangle_N$ (G)
WR 46			
57461.3213	2339	$-199 \pm 88$	$46 \pm 81$
58864.2960	1477	$342 \pm 154$	$-68 \pm 146$
58885.1674	1845	$35 \pm 94$	$-62 \pm 109$
58885.2627	2046	$-43 \pm 99$	$-7 \pm 97$
58892.1191	1189	$268 \pm 194$	$81 \pm 173$
58898.3843	1905	$23 \pm 93$	$-41 \pm 115$
58900.1569	1088	$-112 \pm 160$	$23 \pm 179$
WR 55			
58892.2058	2388	$205 \pm 58$	$-16 \pm 55$
58898.3492	2579	$-378 \pm 85$	$-2 \pm 78$
58900.2075	2168	$56 \pm 80$	$63 \pm 82$
58916.3059	2386	$4 \pm 66$	$-16 \pm 57$
58918.2531	533		

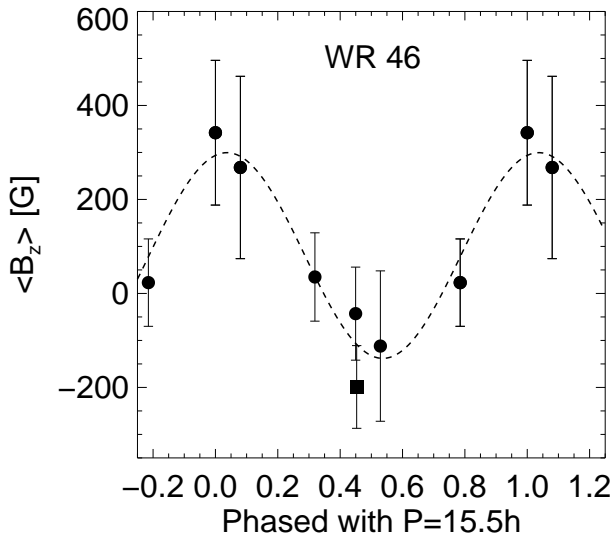


**Figure 3.** Longitudinal magnetic field measurements of WR 46 carried out using low-resolution FORS 2 spectropolarimetric observations and phased with the period of 15.5 h. The overplotted dashed curve corresponds to the sinusoidal fit. The filled square corresponds to the observation obtained in 2016.

square appears (purely coincidentally) slightly shifted from the expected negative field extremum. Interestingly, our period analysis by fitting a sinusoid to the measurements obtained in 2020, indicates almost the same rotation period  $P_{\text{rot}} = 15.53 \pm 0.14$  h. Obviously, the fidelity of the 15.5 h period needs to be confirmed with a long-term extensive data set.

For WR 55, the values for the longitudinal magnetic field  $\langle B_z \rangle$  show change of polarity with the highest field values

$\langle B_z \rangle = -378 \pm 85$  G at a significance level of  $4.4\sigma$  and  $\langle B_z \rangle = 205 \pm 58$  G at a significance level of  $3.5\sigma$ . In view of the importance of the field detection at a significance level of  $4.4\sigma$ , we decided to carry out a consistency check using a different spectral extraction. The parallel and perpendicular beams in the observations at this epoch were extracted using a pipeline written in the MIDAS environment and developed by T. Szeifert, the very first FORS instrument scientist. More details on this pipeline can be found in Hubrig et al. (2014). The result of this measurement,  $\langle B_z \rangle = -334 \pm 77$  G, is fully compatible with the measurement  $\langle B_z \rangle = -378 \pm 85$  G within the error bars.

The simplest model for the magnetic field geometry in stars with globally organized fields is based on the assumption that the studied stars are oblique dipole rotators, i.e. their magnetic field can be approximated by a dipole with the magnetic axis inclined to the rotation axis. Unfortunately, the rotation axis inclination  $i$  for WR stars is undefined because of their dense winds, making the measurement of the projected rotation velocity  $v \sin i$  using broad emission lines impossible. Since the rotation period and the limb-darkening are also unknown for WR 55, we can only estimate for this star a minimum dipole strength of  $\sim 1.13$  kG using the relation  $B_d \geq 3 |\langle B_z \rangle_{\text{max}}|$  (Babcock 1958).

### 3 DISCUSSION

Although magnetic fields are now believed to play an important role in the evolution of massive stars, spectropolarimetric observations of WR stars, which are descendants of massive O stars, are still very scarce. WR stars are usually rather faint, and, in addition, their line spectra are formed in the strong stellar wind, with the wind broadening of the emission lines up to a few thousand  $\text{km s}^{-1}$ . Both WR 46 and WR 55 are faint with visual magnitudes  $m_v \geq 10.9$ , and have never been observed spectropolarimetrically in the past. So far, the presented FORS 2 observations are the first to explore the magnetic nature of these targets. The strongest mean longitudinal magnetic field for WR 46 was measured at a significance level of  $2.2\sigma$  at the positive field extremum and at the level  $2.3\sigma$  close to the negative field extremum. Only for WR 55 we achieve formally definite detections,  $\langle B_z \rangle = -378 \pm 85$  G at a significance level of  $4.4\sigma$  and  $\langle B_z \rangle = 205 \pm 58$  G at a significance level of  $3.5\sigma$ . We should, however, keep in mind that the magnetic field is diagnosed in the line-forming regions, which fall fairly far out in a WR wind, and not at the stellar surface. Different lines form over different zones of the wind, sampling different field strengths. Thus, the method we apply for the measurements only gives a result for the field strength where lines are formed. It is expected that the surface values of the magnetic field are significantly stronger than the field measured in the wind lines (de la Chevrotière et al. 2013).

With respect to the confidence of the field detection, a recent detailed comparison between our analysis technique and an independent analysis from another team showed that the measurement results agree well within expected statistical distributions (Schöller et al. 2017). This gives us high confidence about the accuracy of our longitudinal magnetic field measurements. Importantly, detections at a  $\leq 3\sigma$  level appear to be genuine in a number of studies where the measurements show smooth variations over a rotation period, simi-



lar to those found for the magnetic Of?p stars HD 148937 and CPD  $-28^{\circ}$  2561 (Hubrig et al. 2008, 2011, 2013, 2015). In these studies, not a single reported detection reached a  $4\sigma$  significance level.

The first detection of the presence of a magnetic field in WR 55 makes this star the best candidate for long-term spectropolarimetric monitoring. Future observing campaigns should be based on spectropolarimetric time series to further strengthen the evidence for the magnetic nature of this star and to set more stringent limits to its magnetic field strength. The temporal variations of the measured longitudinal magnetic fields should be used to ascertain the rotation/magnetic period of WR 55 and determine for the first time the geometry of the global magnetic field in a WR star.

Furthermore, the detection of the magnetic field in WR 55 associated with the ring nebula RCW 78 and its molecular environment is of an exceptional importance for our understanding of star formation. According to Cappa et al. (2009), WR 55 is not only responsible for the ionization of the gas in the nebula, but also for the creation of the interstellar bubble. The presence of star formation activity in the environment of this nebula suggests that it may have been triggered by the expansion of the bubble.

## ACKNOWLEDGEMENTS

Based on observations made with ESO Telescopes at the La Silla Paranal Observatory under the programme IDs 097.D-0428(A) and 0104.D-0246(A). SPJ is supported by the German Leibniz-Gemeinschaft, project number P67-2018. We thank the referee G. Mathys for his constructive comments.

## DATA AVAILABILITY

The FORS2 data from 2016 are available from the ESO Science Archive Facility at <http://archive.eso.org/cms.html>. The data from 2020 will become available in March 2021 at the same location and can be requested from the author before that date.

## REFERENCES

Angel J. R. P., Landstreet J. D., 1970, *ApJ*, 160, L147  
 Appenzeller I., et al., 1998, *The ESO Messenger*, 94, 1  
 Babcock H. W., 1958, *ApJS*, 3, 141  
 Cappa C. E., Rubio M., Martín M. C., Romero G. A., 2009, *A&A*, 508, 759  
 Chené A.-N., St-Louis N., 2011, *ApJ*, 736, 140  
 Cikota A., Patat F., Cikota S., Faran T., 2017, *MNRAS*, 464, 4146  
 Conti P. S., Massey P., 1989, *ApJ*, 337, 251  
 de la Chevrotière A., St-Louis N., Moffat A. F. J., MiMeS Collaboration, 2013, *ApJ*, 764, 171  
 de la Chevrotière A., St-Louis N., Moffat A. F. J., MiMeS Collaboration, 2014, *ApJ*, 781, 73  
 Gayley K. G., Ignace R., 2010, *ApJ*, 708, 615  
 Gosset E., De Becker M., Nazé Y., Carpano S., Rauw G., Antokhin I. I., Vreux J.-M., Pollock A. M. T., 2011, *A&A*, 527, A66  
 Grunhut J. H., et al., 2017, *MNRAS*, 465, 243  
 Hamann W.-R., Gräfener G., Liermann A., 2006, *A&A*, 457, 1015  
 Hamann W.-R., et al., 2019, *A&A*, 625, A57

Hénault-Brunet V., St-Louis N., Marchenko S. V., Pollock A. M. T., Carpano S., Talavera A., 2011, *ApJ*, 735, 13  
 Hubrig S., Kurtz D. W., Bagnulo S., Szeifert T., Schöller M., Mathys G., Dziembowski W. A., 2004a, *A&A*, 415, 661  
 Hubrig S., Szeifert T., Schöller M., Mathys G., Kurtz D. W., 2004b, *A&A*, 415, 68  
 Hubrig S., Schöller M., Schnerr R. S., González J. F., Ignace R., Henrichs H. F., 2008, *A&A*, 490, 793  
 Hubrig S., et al., 2011, *A&A*, 528, A151  
 Hubrig S., et al., 2013, *A&A*, 551, A33  
 Hubrig S., Schöller M., Kholtygin A. F., 2014, *MNRAS*, 440, L6  
 Hubrig S., et al., 2015, *MNRAS*, 447, 1885  
 Hubrig S., et al., 2016, *MNRAS*, 458, 3381  
 Michaux Y. J. L., Moffat A. F. J., Chené A.-N., St-Louis N., 2014, *MNRAS*, 440, 2  
 Mullan D. J., 1984, *ApJ*, 283, 303  
 Ramiaramanantsoa T., et al., 2014, *MNRAS*, 441, 910  
 Schöller M., et al., 2017, *A&A*, 599, A66  
 St-Louis N., Dalton M. J., Marchenko S. V., Moffat A. F. J., Willis A. J., 1995, *ApJ*, 452, L57  
 Steffen M., Hubrig S., Todt H., Schöller M., Hamann W.-R., Sandin C., Schönberner D., 2014, *A&A*, 570, A88  
 Thompson T. A., Chang P., Quataert E., 2004, *ApJ*, 611, 380  
 Veen P. M., Van Genderen A. M., Crowther P. A., van der Hucht K. A. 2002a, *A&A*, 385, 600  
 Veen P. M., Van Genderen A. M., van der Hucht K. A. 2002b, *A&A*, 385, 619

This paper has been typeset from a  $\text{\TeX}/\text{\LaTeX}$  file prepared by the author.